Considerations Regarding the Relationship between Power Factor and Harmonic Distortions of Switched Mode Power Supplies

Attila Buchman[1], Claudiu Lung[2]
[1]University of Debrecen, Faculty of Informatics, Debrecen, Hungary
[2]Technical University of Cluj-Napoca, North University Center of Baia-Mare, Romania
abuchman@ubm.ro

***Abstract*-The main goal of this paper is to present some experimental results regarding power factor (PF) and current total harmonic distortions (THDi) of some very common loads on low voltage a.c. lines i.e. the power supply of computers, monitors and TV sets. The causes of some unexpected values are investigated and some physically meaningful explanations are delivered. The impact of the output current value on PF is emphasized thus proving that one single PF value cannot fully qualify a SMPS. It is also proven that harmonic analysis based THDi values may be very misleading if inter-harmonic components are neglected. Finally an old concept, of renewed interest, the dependency of THDi on PF is revisited.**

INTRODUCTION

As nonlinear loads become more and more prevalent, the effect on the power system becomes increasingly pronounced. Harmonic components are injected back into the system and the resulting voltage drops across the source impedance creates voltage distortion in the power system. Figure 1 shows the wiring system of a typical commercial office building, along with its voltage harmonic distortions under mixed, linear and nonlinear loads. The most significant harmonic producers in this system are the switch-mode power supplies (SMPS) used in PCs and other appliances [1].

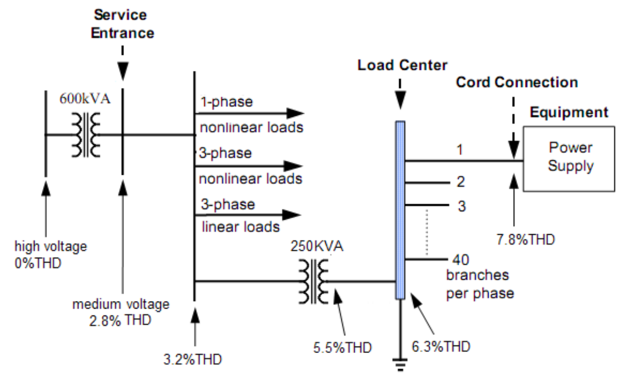

Fig. 1. Typical commercial or office building distribution system (values and schematic based on [1]).

In fact, each SMPS uses a rectifier to connect to the a.c. line. Common rectifiers have smoothing capacitors to reduce voltage ripple. These capacitors charges for a very short period of time close to the moment when the mains voltage reaches its maximum value. One can say that all rectifiers connected to the same phase of the a.c. line charge their capacitors at the same time. That is the main reason for the flat-topping of the mains voltage on all a.c. lines heavily loaded whit common electronic appliances (personal computers, monitors, TV sets). A total harmonic distortion of 6% to 8% is expectable at the cord connection point. A typical shape for the voltage in most office building's wall socket is shown in fig.2.

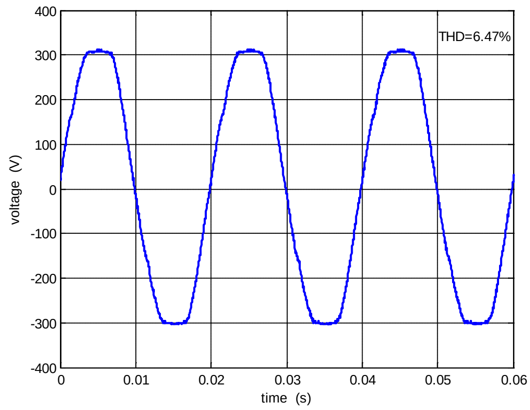

Fig. 2. Mains voltage waveform at wall socket in North University of Baia Mare main building (THD value is 6.47%).

It is obvious (looking at fig.2) that one can speak about non-sinusoidal voltage here. The frequency spectrum of the voltage (fig.3) confirm this fact. Harmonics are causing equipment to be subjected to voltages and currents at frequencies for which it was not designed. The effects of such exposure may not be instantly visible but can have serious consequences in the medium and long term [3].

The most important step in order to reduce voltage distortions is to reduce current harmonics generated by non linear loads. In this respect it is important to investigate how well classical power quality indices (PF, THDi) qualify a load under non-sinusoidal voltage condition. The first step would be to define these indices according to one well accepted power theory.

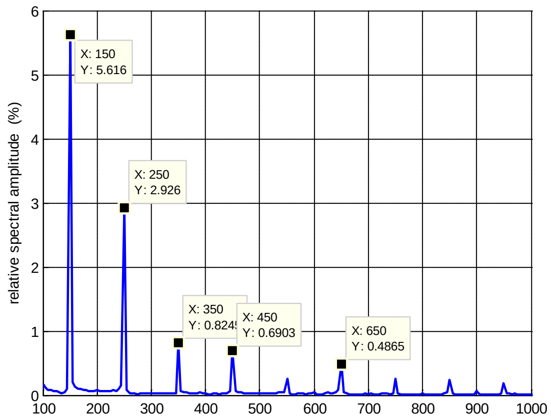

Fig. 3. Frequency spectrum for the waveform in fig. 2. The fundamental component amplitude (not reprezented) is 100%.

IEEE GROUP POWER THEORY

This power theory developed mainly with contributions due to Filipski [4] and Emmanuel [5]. The concept presented in [6] is based on the assumption that the goal of electrical energy transmission is to deliver as much of power as possible at the fundamental frequency. Since energy transfer at harmonic frequencies also occur, it makes sense to separate the fundamental and the harmonic components from each other. Using the rms values of voltage (U) and current (I) equations (1) and (2) can be written.

$$U^2 = U_1^2 + U_H^2 \tag{1}$$

$$I^2 = I_1^2 + I_H^2 \tag{2}$$

$$U_H^2 = \sum_{n\neq 1} U_n^2 \tag{3}$$

$$I_H^2 = \sum_{n\neq 1} I_n^2 \tag{4}$$

U_1 and I_1 refers to the rms of the fundamental components of voltage and current while U_H and I_H are defined in (3) and (4), with n representing harmonic order.

The apparent power (S) is also decomposed into a fundamental (S_1) and a non-fundamental (S_N) component (eq.5)

$$S^2 = S_1^2 + S_N^2 \tag{5}$$

$$S_1^2 = (U_1 \cdot I_1)^2 = P_1^2 + Q_1^2 \tag{6}$$

$$S_N^2 = (U_1 \cdot I_H)^2 + (U_H \cdot I_1)^2 + (U_H \cdot I_H)^2 \tag{7}$$

Multiplying (1) and (2) and comparing the result to (5), S_1 and S_N can be expressed as in (6) and (7).

The fundamental apparent power (6) can be further resolved into the fundamental active power (P_1) and fundamental reactive power (Q_1) according to the well-known equation used under pure sinusoidal conditions.

The non-fundamental apparent power (7) has three components:

(i). $(U_1 \cdot I_H)^2$ or current distortion power;
(ii). $(U_H \cdot I_1)^2$ or voltage distortion power;
(iii). $(U_H \cdot I_H)^2 = S_H^2$ or harmonic apparent power;

The ratio of S_N and S_1 is the normalized non-fundamental distortion power (eq.8).

$$\left(\frac{S_N}{S_1}\right)^2 = \left(\frac{I_H}{I_1}\right)^2 + \left(\frac{U_H}{U_1}\right)^2 + \left(\frac{I_H}{I_1}\right)^2 \cdot \left(\frac{U_H}{U_1}\right)^2 \tag{8}$$

Total harmonic distorsions of current and voltage can now be defined as in (9) and (10) and (8) rewritten as (11).

$$THDi^2 = \left(\frac{I_H}{I_1}\right)^2 = \frac{\sum_{n\neq 1} I_n^2}{I_1} \tag{9}$$

$$THDu^2 = \left(\frac{U_H}{U_1}\right)^2 = \frac{\sum_{n\neq 1} U_n^2}{U_1} \tag{10}$$

$$\left(\frac{S_N}{S_1}\right)^2 = THDi^2 + THDu^2 + THDi^2 \cdot THDu^2 \tag{11}$$

As one can see, the normalized non-fundamental distortion power includes the effect of all sort of harmonic distortion and is therefore, a very good power quality index.

As S_1 in (6), S_H too is the sum of two terms (12)

$$S_H^2 = P_H^2 + N_H^2 \tag{12}$$

Thus, an active (P_H) and a non-active (N_H) harmonic power are introduced. Their sum is the active power (P). Now, a total power factor or true power factor can be defined as in (13). The adjective ‘true’ emphasizes the fact that PF is not equivalent to ‘$cos\varphi$’ as it were under pure sine source voltage and linear load condition. Under distorted voltage and non-linear loading condition $cos\varphi$ is the fundamental power factor (PF_1), as defined in (14).

$$PF = \frac{P_1 + P_H}{S} = \frac{P}{S} \tag{13}$$

$$PF_1 = \frac{P_1}{S_1} = cos(\varphi_1) \tag{14}$$

According to (13) and (14) PF and PF_1 can be computed only if the spectral components of voltage and currents are known. Still the active power is defined in time domain (15). This is in fact the only definition common to all power theories.

$$P = \frac{1}{k \cdot T} \cdot \int_{\tau}^{\tau + kT} p \cdot dt \tag{15}$$

In (15) p is the instantaneous power, T is the fundamental period, τ is the time instant when the observation begins and k is the number of periods observed. Under strictly periodical conditions k is irrelevant and one could ask why was introduced (in the ‘classical’ definition $\tau=0$ and $k=1$). The truth is that in real world no such thing as two identical periods exists. Extending the observation interval over a large number of periods is a straightforward method to reject random noise. According to actual regulations observation time should be at least *200ms* i.e. $k \geq 10$.

POWER QUALITY INDICES

The first, step toward power-quality measurement is the definition of power-quality indices able to quantify the deviation from an ideal reference situation. A quite natural way seems to be the extension to the non-sinusoidal conditions of the indices employed under sinusoidal conditions, such as the power factor and the total distortion factor (THD), together with a discussion of their limits when the sinusoidal conditions are left [7].

1. *Power factor*

The power factor (13) can still be considered a power-quality index, though it loses the property of fully qualifying the load. Under non-sinusoidal conditions it only represents an index of conformity of the line current waveforms to the line voltage waveforms [7]. As experimental results will prove *PF* is a good quality index if *THDi* is large compared to *THDu*. In fact *PF=1* means no more than voltage and currents are proportional i.e. equally distorted. If the current were less distorted than the voltage *PF* would be less than 1 although the load's current is more 'sine like'.

The main reason for *PF* to be used as a power quality index is that it can be computed based on a few simple measurements.

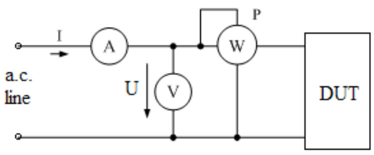

Fig. 4. Basic measurement setup for power factor computation. .

The basic experimental setup for power factor computation is shown in fig.4. The device under test (DUT) is connected to the line while a true rms ampere (A) and volt (V) meters monitor the effective values of current and voltage respectively. A wattmeter (W) is used to measure active power. It takes two readings (*U* and *I*) to compute *S* and one more reading (*P*) to compute *PF* according to (13).

Another approach is to record *n* samples of the instant values of voltage (*v*) and current (*i*) for a number of *k* periods of mains voltage. Using these samples, *U*, *I*, *S*, *P* and finally *PF* can be computed, using (16)-(19) and (13) respectively.

$$U^2 = \frac{1}{n} \cdot \sum_{i=1}^{n} v_i^2 \quad (16)$$

$$I^2 = \frac{1}{n} \cdot \sum_{i=1}^{n} i_i^2 \quad (17)$$

$$S^2 = U^2 \cdot I^2 \quad (18)$$

$$P = \frac{1}{n} \cdot \sum_{i=1}^{n} (v_i \cdot i_i) \quad (19)$$

Although fairly simple, this method implies a square root extraction in order to compute *S* from (18). A division is also required to compute *PF* from (*10*). These are computationally demanding algorithms to implement on a microcontroller (MCU). The computing power of a digital signal processor (DSP) is required for a proper hardware implementation of the method. Many commercially available clamp meters use an embedded system which includes MCU and DSP as well to perform real time readings and data recording as well.

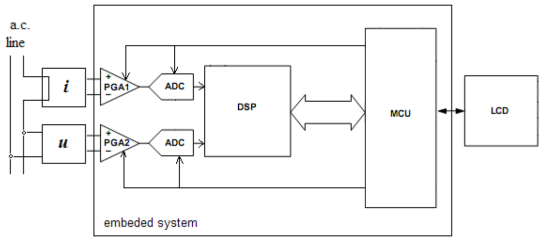

Fig. 5. Block diagram of an embedded system capable of PF computing

Figure 5 presents a block diagram of such a system. A voltage divider (u) and a current sensor (i) interfaces the a.c. line with the embedded system, usually providing galvanic insulation as well. On the other end an LCD displays the results. The MCU sets the gain for the programmable gain amplifiers (PGA), triggers the analog to digital converters (ADC), controls and reads the results from DSP and updates the LCD display.

2. *Total harmonic distortions*

If, as was stated in the previous subsection, *PF = 1* does not necessarily yields zero harmonic contents, *THDi=0* and *THDu=0* would certainly imply that. So, being strictly related to harmonic distortions, these parameters can be successfully used as power quality indices. The only major drawback concerning their usage is that neither of them can be directly measured or computed in time domain. A spectral analysis is required to compute them, and this is a time and computing resources demanding task.

However, using both of them not only indicates the level of harmonic pollution, but also indicates if the load under test contributes to that pollution. Indeed, if the load were purely resistive, THDi and THDu would be equal. By consequence, if THDi is larger than THDu the load is non-ideal and thus polluting.

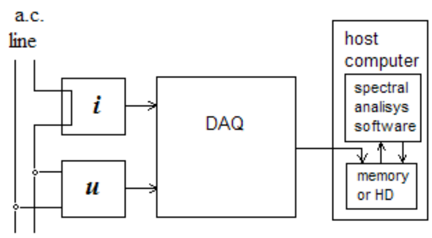

Fig. 6. Experimental setup for total harmonic distorsions computing

Figure 6 shows an experimental setup that can be used for spectral analysis and time domain computations as well. Instead of an embedded system a general purpose two channel data acquisition module (DAQ) connected to a host computer is employed. Once sampled, *i* and *u* are stored as two data records in the memory or on the hard disk (HD) of the host. It's now up to the software running on the computer to perform whatever computations on these strings of data, spectral analysis included.

3. Fundamental power factor

Fundamental power factor, as defined in (14) does not includes harmonic related terms. That is why PF_1 is not a power quality indicator under non-sinusoidal conditions. As our experiments will prove it is in fact very close to unity for SMPS even for those who has no power factor correction (PFC) at all. Frequency domain analysis is needed to compute this factor. That is a disadvantage, compared to *PF*. Both the above mentioned reasons explains why when it comes to SMPS power quality indices, PF_1 is not mentioned at all.

EXPERIMENTAL RESULTS

In order to test the ability of the indices defined in the previous section to qualify loads according to their impact on the power quality, several measurements, on six of the most popular a.c. loads were performed. Table I enumerates them all. The last column refers to the built in power factor correction methods. The experimental setup was the same as in fig.6.

TABLE I
LIST OF POWER SUPPLIES UNDER TEST

Notation	Description	PFC
SMPS1	Low power (12W), general purpose a.c. adapter	none
SMPS2	CRT television set	passive
SMPS3	LCD monitor	passive
SMPS4	Desktop PC	passive
SMPS5	Energy Star Compliant CRT monitor	active
SMPS6	Medium power (150W) general purpose power supply	active
SMPS7	Color laser printer	active

1. Current and voltage sensing

As current sensor, a current transformer was used. The initial volt per amp ratio was *0.1V/A* for *100Ω* load and one primary turn (fig.7). In order to increase the sensitivity of this sensor 20 primary turns were used thus increasing the volt per amp ratio to *2V/A* on *100Ω* load.

Voltage sensing is more an issue of galvanic isolation from the mains. A transformer and a voltage divider were used to adjust the voltage level and protect the input to the DAQ. A total ratio of *1/90* between the DAQ input and the mains voltage was set.

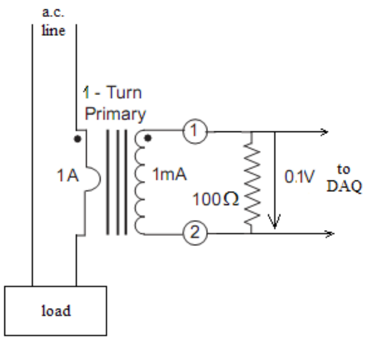

Fig. 7. Current transformer connection and typical parameters

2. Data acquisition system

A commercially available two channel, 8 bit resolution DAQ module was used. It had 50MHz maximum sampling rate and a 32kB data buffer on each channel. It was connected to a host computer using its own data acquisition and data logging software. This software allowed us to store data into ASCII formatted text files.

The observation period was set to 200ms i.e. 10 full periods of mains voltage. A sampling rate of 100kHz was set, thus enabling the storage of 20,000 samples during the observation period.

3. Data processing algorithm

On the host computer a Matlab script was created in order to load the recorded data, perform the time and frequency domain computations, store and display the results. This script assumes that the data is recorded in a three column format, the first column being the time record (sampling moments in nanoseconds), the second the voltage record and the last column must contain the samples of the current. If this format is respected, the only input for the Matlab script is the name of the data file.

Running the script, the data file is loaded and the length (n) of the record is derived. Then, assuming uniform sampling interval, the sampling frequency (f_S) is computed. These values set the frequency resolution of the spectral analisys. As previously stated in subsection 2, in our experiments $n=20{,}000$ and $f_S=100kHz$. These values would give for the spectrum a frequency resolution of $f_S/n = 5Hz$.

4. Results

Table II presents the *PF*, *THDI*, *THDu*, and PF_1 values computed for the seven SMPS under test.

TABLE II
POWER QUALITY INDICES FOR THE SMPS'S UNDER TEST

Load	PF [%]	$THDi_1$ [%]	$THDi_2$ [%]	THDu [%]	PF_1
SMPS1	52.11	134.65	134.67	6.47	0.9256
SMPS2	68.12	98.07	98.08	7.08	0.9948
SMPS3	72.93	79.63	79.65	8.17	0.9867
SMPS4	81.91	67.79	67.82	9.18	0.9952
SMPS5	97.12	22.31	22.32	8.36	0.9979
SMPS6	93.58	13.70	17.82	6.19	0.9935
SMPS7	79.27	5.59	51.44	8.49	0.9906

As one can see there are two columns for THDi. The first of them contains THDi values computed using only the harmonic components of the current, i.e. those who are a multiple of 50Hz. This method gives an incredibly low value for SMPS7 (a printing laser printer). It is unlikely that THDi is lover than THDu. In order to address this issue the amplitude spectrum of the current was printed (fig.8). It is obvious that significant amplitude components are located at 25Hz and multiple of this sub-harmonic frequency (inter-harmonics).

The forth column in table II shows the THDi values if one takes into account this sub and inter-harmonics components to. There is an excellent match between columns three and forth in table II, except for SMPS7 where 51.44 seems to be the true value. In order to validate this hypothesis an approximate value for THDi was computed from (18). Although (20) holds only under sinusoidal voltage condition, taking into account that the voltage is less then 10% distorted, we might expect that (18) would provide THDi with something like 10% error.

$$THDi^2 = \frac{PF_1^2}{PF^2} - 1 \qquad (20)$$

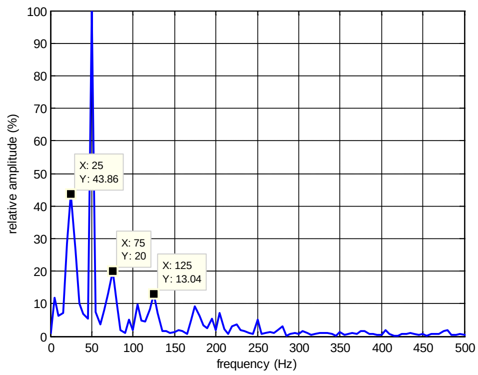

Fig. 8. Relative amplitude spectrum for the current of SMPS7

Table III presents *THDi* values computed with (20). The relative errors versus $THDi_1$ and $THDi_2$ computed according to (21) are presented in the last two columns.

$$\varepsilon_{rk} = \frac{THDi_3 - THDi_k}{THDi_3}, \; k = 1 \cup k = 2 \qquad (21)$$

As one can see, $\varepsilon_{r2} < \varepsilon_{r1}$ so $THDi_2$ seems to be a better estimate for *THDi* than $THDi_1$. In the last section of the paper, more remarks will be made on this issue.

TABLE III
COMPUTED VALUES FOR THDI

Load	PF [%]	PF1	$THDi_3$ [%]	ε_{r1} [%]	ε_{r2} [%]
SMPS1	52.11	0.9256	146.80	8.27	8.26
SMPS2	68.12	0.9948	106.42	7.84	7.83
SMPS3	72.93	0.9867	91.12	12.60	12.58
SMPS4	81.91	0.9952	69.00	1.75	1.71
SMPS5	97.12	0.9979	23.61	5.51	5.46
SMPS6	93.58	0.9935	34.73	60.55	48.69
SMPS7	79.27	0.9906	74.94	92.54	31.35

Tabel IV presents the results of another set of measurement: the dependency of *PF* and *THDi* to the output current (I_L) of SMPS6. The current drawn from this supply was increased from *1A* to *10A* in *0.5A* increments, and then decreased in the same manner to *1A*.

As one can see, for low output currents, SMPS6 act as if it has no PFC at all, with PF values similar to SMPS1. It takes a certain threshold to be passed for PFC to operate and thus *PF* approaches unity. Once up and running, PFC circuitry will stop only if the output current decreases under a threshold that is much lower than that at which has started. As figure 9 clearly shows, *PF* has a hysteretic behavior with respect to I_L

TABLE IV
PF AND THDI COMPUTED FOR SEVERAL VALUE OF I_L

I_L [A]	PF [%]	$THDi_2$ [%]	I_L [A]	PF [%]	$THDi_2$ [%]
1.0	44.13	132.31	10	91.18	21.044
1.5	49.49	136.01	9.5	91.68	18.252
2.0	53.34	132.97	9.0	92.08	20.644
2.5	57.15	125.97	8.5	92.01	18.363
3.0	58.43	124.74	8.0	92.64	17.783
3.5	60.30	118.59	7.5	93.34	15.781
4.0	62.36	111.71	7.0	93.20	15.974
4.5	66.57	97.885	6.5	93.32	16.215
5.0	66.51	98.725	6.0	93.50	14.436
5.5	64.30	105.88	5.5	94.09	10.877
6.0	66.39	99.558	5.0	95.16	9.7666
6.5	66.37	99.184	4.5	77.78	18.348
7.0	93.85	14.705	4.0	81.81	21.47
7.5	93.53	15.952	3.5	74.65	20.067
8.0	92.97	16.948	3.0	74.38	18.683
8.5	92.97	17.602	2.5	56.56	128.89
9.0	92.33	19.329	2.0	55.03	131.48
9.5	91.57	20.391	1.5	50.80	134.48
10	91.18	21.044	1.0	46.00	133.66

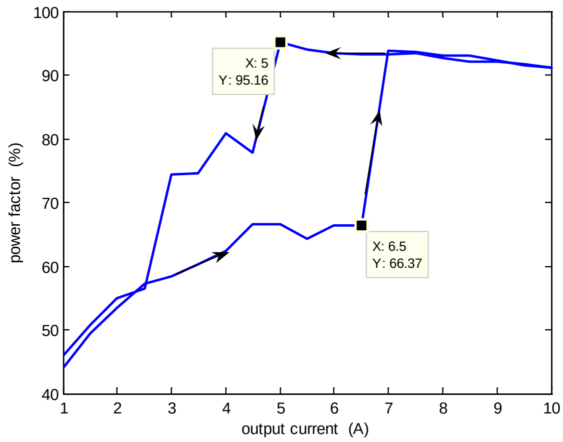

Fig. 9. Power factor versus load current for SMPS6

CONCLUSIONS

All seven SMPS's under test were measured in their usual operating condition, neither in idle state nor under heavy load condition (except for SMPS6 which was accessible for this type of investigation). Several conclusions can be drawn from the experimental results presented in table II.

(1). When no PFC is present, (SMPS1 in table II) the *PF* value is worst then that of an ordinary full wave rectifier. Figure 10 provides an explanation to this fact. As one can see, the current drawn by the source has two components. Besides the current spikes due to the rectifier's output capacitor charging a sine shaped, 90^0 out of phase, current is also visible. This is due to the fact that all SMPS have a so called line filter at their input in order to limit the propagation of the switching frequency harmonics towards the a.c. line. A typical line filter is presented in fig. 11. One can see a capacitor (C) in parallel with the a.c. line. The current thru this capacitor explains the sine shaped component of the input current. The 90^0 phase angle between this current and the mains voltage explains the degradation of the power factor. Another consequence of this fact is that SMPS1 has the lowest PF_1 value. These phenomena are less visible as the output current of the SMPS increase and the current absorbed by the rectifier becomes large compared to the capacitive component.

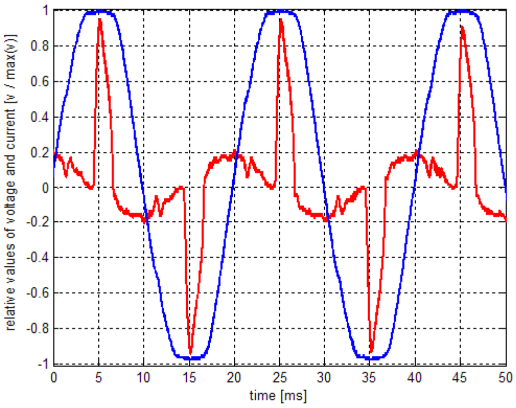

Fig. 10. Input voltage and current waveforms for SMPS1

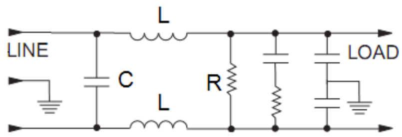

Fig. 11. Typical RFI power line filter schematic

(2). When comparing $THDi_1$ and $THDi_2$ columns in table II one can see a very good match between the two values suggesting that the input current has only harmonic (integer multiples of mains frequency) components. In fact that depends again on the output current of the SMPS. If the current drawn from the SMPS is relatively stable or varies slowly the current consumed from the mains will have only harmonic component, more than that, only odd harmonics (fig.12). On the contrary, if the current drawn from the SMPS is rapidly pulsing from low to high values (as for SMPS7 which supplies a printing laser printer) then sub-harmonic and inter-harmonic components appear, as in fig. 8. The explanation is simple if one looks at the current waveform in figure 13. Five periods (T1…T5) of 40ms each, of a pseudo-periodic signal are visible in the 200ms wide observation window. This means a fundamental frequency of *1/0.04=25Hz* for this waveform. Related to the mains frequency this is a sub-harmonic component and its multiples produce the inter-harmonic components in fig.8. That is the reason why $THDi_1$ and $THDi_2$ does not match (table II).

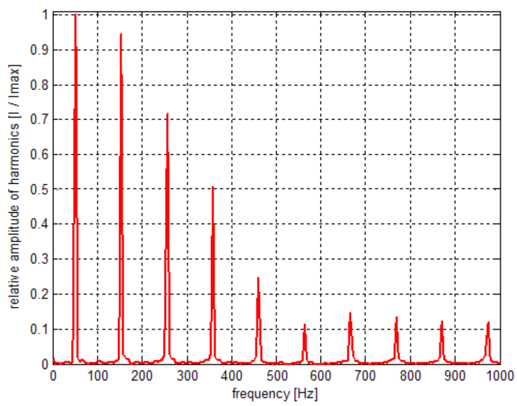

Fig. 12. Relative amplitude spectrum of input current for SMPS1

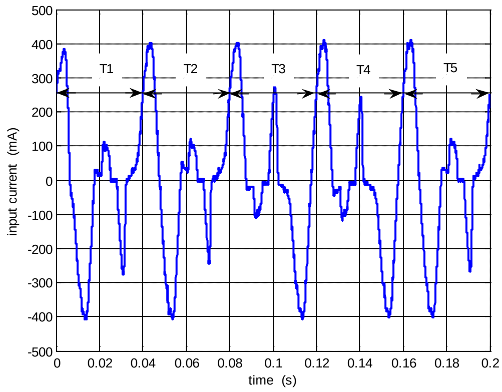

Fig. 13. Input current waveform for SMPS7

(3). Even if one ignores the SMPS7 row in table II still *THDi* does not decrease as *PF* increases. One can see that although SMPS5 has better *PF* than SMPS6, the later has lower *THDi*. The graph of $THDi_1$ and $THDi_2$ versus *PF* (fig.14) shows this fact clearly. This result is not so confusing if we take into account that *THDi* and *PF* quantifies two slightly different things. *THDi* is a measure of the resemblance between the current and a pure sine wave (of the same frequency as the mains voltage). On the other hand *PF* is a measure of the resemblance between the current and the mains voltage. Since the mains voltage itself is distorted (see *THDu* column in tab.II) it's just possible that one current resembles more to the voltage and the other to a pure sine. To further investigate this possibility the waveforms of the currents are presented in fig.15 and fig.16 and their amplitude spectrums in fig.17 and fig.18 respectively.

Comparing the two current waveforms it is obvious that the two SMPS have different PFC strategies. While for SMPS5 the current seems to fallow the distorted mains voltage (fig.15) for SMPS6 that is not obvious at all. In fact only the mean value of this current seams sine wave shaped. The high frequency noise visible in fig.16 is due to the active PFC circuit switching. A better line filter would certainly reduce this noise. But, as noisy as it is, it has a better harmonic content then SMPS5's current (fig.17).

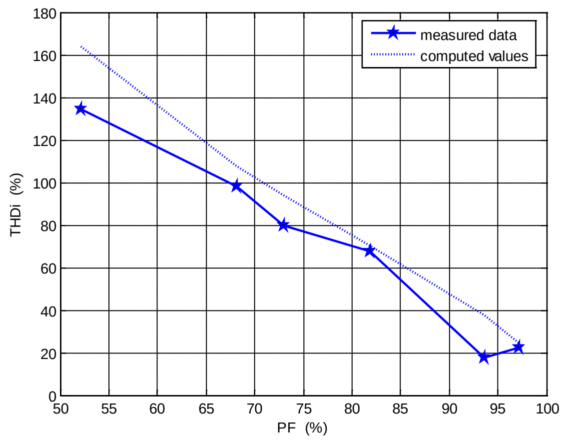

Fig. 14. Three graphs representing THDI versus PF. Measured data in the graph's legend refers to values computed in frequency domain while computed data refers to values computed in time domain, using cos(φ)=1 in (18).

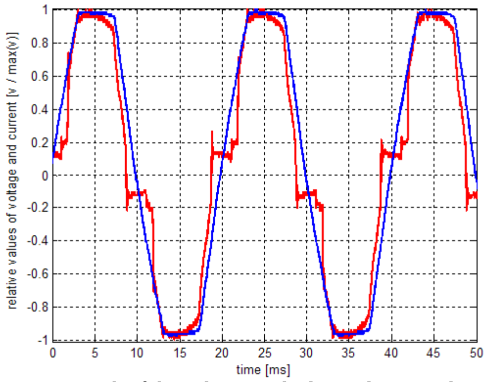

Fig. 15. Graph of the voltage applied to and current drawn by SMPS5 in relative units.

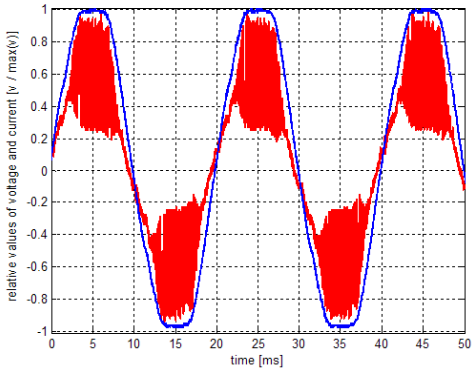

Fig. 16. Graph of the voltage applied to and current drawn by SMPS6 in relative units.

The effect of the switching noise and its sub-harmonics is visible in fig.18. While SMPS5 has all its spectral line well under 0.5% relative amplitude, some spectral lines of SMPS6 are well above 1%, the one at 8110 Hz reaching almost 3.5%. It worth noticing that 8110Hz is not a multiple of 50Hz so it must be an inter-harmonic component produced by the PFC circuit.

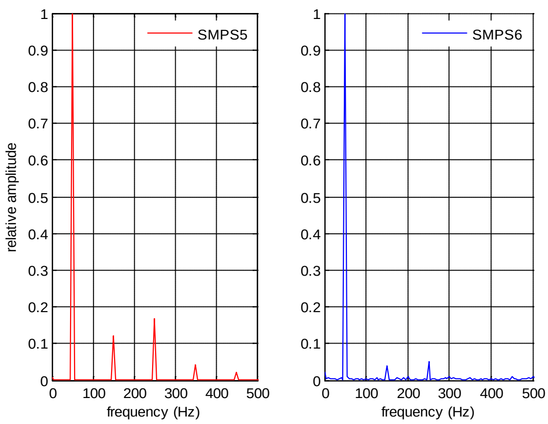

Fig. 17. Spectrum of the current drawn by SMPS5 and SMPS6 in a low frequency range (0 – 500Hz).

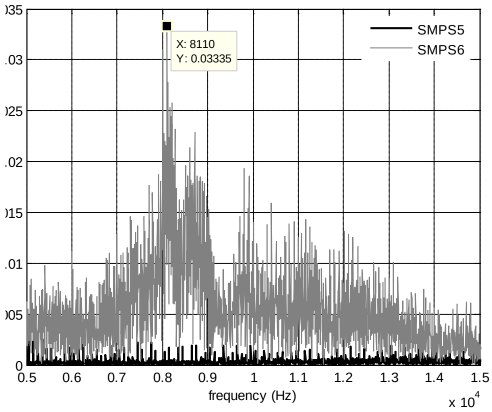

Fig. 18. Comparison between the spectrums of SMPS5 and SMPS6 in a higher frequency interval (5000 Hz – 15000Hz)

(4). The *THDu* column in table II shows different values because the measurements were made at different time and different locations. It is unlikely that one particular load would influence this value. But the truth is that thousands of them would certainly do. In fact, these high values of *THDu* in office buildings are mainly attributable to the huge number of monitors and computers drawing more or less non-sinusoidal currents.

(5). The last column in table II confirms the fact that *PF1* is no longer a valid power quality index. Moreover, his value seems to be 1. That is useful information because *PF1* is the only term in (20) that is frequency dependent. Substituting *PF1=1* in (20) allows the estimation of *THDi* without any spectral analysis (that holds for SMPS of course).

$$THDi^2 = \frac{1}{PF^2} - 1 \qquad (22)$$

As table III and figure 14 clearly illustrates, the measured and estimated values gives a good fit especially for high *PF* values. Table III shows that the worst fit appears for SMPS6 and SMPS7, both having inter-harmonic components in their spectrum. The frequency domain analysis was extended only to inter-harmonics being a multiple of 25Hz. To investigate other inter-harmonics would be misleading, taking into account that the sample number and the sampling frequency set a 5Hz limit for the spectral resolution. Under these circumstances there is no reason to assume that the result obtained in frequency domain is better that that computed in time domain.

Extending the investigation on this matter, SMPS6 was tested under several values of loading current (i.e. power factor). Table IV and figure19 presents these results. It is an obvious similarity in the shapes of the two graphs in fig.19. But more experiments should be carried out in order to establish which of them gives the best estimate for THDi.

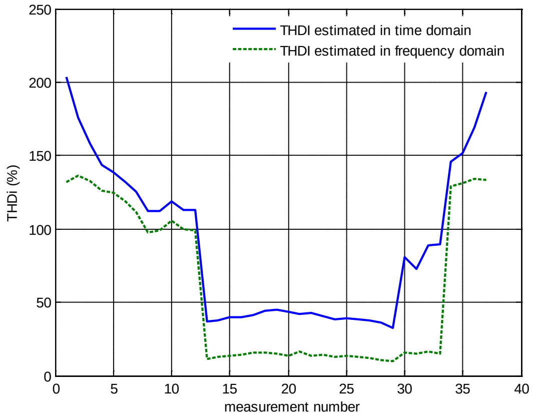

Fig. 19. Comparison between the THDi values computed in time and frequency domain at different load current values

The final conclusion of our work would be that unless a very high resolution frequency domain analysis is perform, *PF* can be used to estimate THDI to, using (22). Using this approximation only time domain analysis is required to qualify the power quality behavior of a SMPS. In this way PF alone is enough to fully qualify a SMPS. But we would also emphasize that only one PF value has no real significance since PF heavily depends on the current drawn from the SMPS.

REFERENCES

[1] Fortenbery, B., Koomey, J., G., *Assessment of the Impacts of Power Factor Correction in Computer Power Supplies on Commercial Building Line Losses*, Power Factor Report CEC 500, March 31, 2006, pp.7-9, www.efficientpowersupplies.org.

[2] Burchall, M., *Harmonic Current Standards - The End of the Line?* The Electricity Association, EMCTLA meeting 19th May 2000.

[3] Bachry, A., *Power Quality Studies in Distribution Systems Involving Spectral Decomposition*, Dissertation zur Erlangung des akademischen Grades Doktoringenieur, Otto-von-Guericke-Universität Magdeburg, 2004

[4] Filipski, P., S., *Apparent Power – A misleading Quantity in the Non-sinusoidal Power Theory: Are all Non-Sinusoidal Power Theories Doomed to Fail?* European Transactions on Electrical Power Engineering ETEP, 1993, Vol. 3, No. 1, pp. 21-26.

[5] Emmanuel, A., E., *The Buchholz-Goodhue Apparent Power Definition, The practical Approach for Nonsinusoidal And Unbalanced Systems.* IEEE Transactions on Power Delivery, April 1998, Vol. 13, No. 2, pp. 344-350.

[6] IEEE Working Group on Nonsinusoidal Situations, *Practical Definitions for Powers in System with Nonsinusoidal Waveforms and Unbalanced Loads: A Discussion.* IEEE Transactions on Power Delivery, Jan. 1996, Vol. 11, No. 1, pp. 79-101.

[7] Ferrero, A., *Measuring electric power quality: Problems and perspectives.* Measurement, Volume 41, Issue 2, Feb. 2008, pp 121-129

[8] ***, *AC1010: 10 Amp Current Transformer*, Datasheet, http://www.talema-nuvotem.com

[9] Chi, K., Tse, *Circuit Theory and Design of Power Factor Correction Power Supplies*, IEEE Distinguished Lecture 2005, http://chaos.eie.polyu.edu.hk.

[10]Czarnecki.L.,S, *Harmonics and power phenomena*, Weley Enceclopidia of Electrical And Electronics Engineering, John Wiley and Sons Inc., Supplement 1. pp.195-218,2000.

[11]Czarnecki.L.,S, *Currents Physical Components in Circuits with Nonsinusoidal Voltages and Currents''. Part 1: Single Phase Linear Circuits*, Electric Power Quality and Utilisation Journal, vol. XI, n° 2, pp: 3-14, 2005.